

Why does neutron transfer play different roles in sub-barrier fusion reactions $^{32}\text{S}+^{94,96}\text{Zr}$ and $^{40}\text{Ca}+^{94,96}\text{Zr}$?

V.V.Sargsyan^{1,2}, G.G.Adamian¹, N.V.Antonenko¹, W. Scheid³, and H.Q.Zhang⁴

¹*Joint Institute for Nuclear Research, 141980 Dubna, Russia*

²*International Center for Advanced Studies,*

Yerevan State University, M. Manougian 1, 0025, Yerevan, Armenia

³*Institut für Theoretische Physik der Justus-Liebig-Universität, D-35392 Giessen, Germany*

⁴*China Institute of Atomic Energy, Post Office Box 275, Beijing 102413, China*

(Dated: December 5, 2021)

Abstract

The sub-barrier capture (fusion) reactions $^{32}\text{S}+^{90,94,96}\text{Zr}$, $^{36}\text{S}+^{90,96}\text{Zr}$, $^{40}\text{Ca}+^{90,94,96}\text{Zr}$, and $^{48}\text{Ca}+^{90,96}\text{Zr}$ with positive and negative Q -values for neutron transfer are studied within the quantum diffusion approach and the universal fusion function representation. For these systems, the s -wave capture probabilities are extracted from the experimental excitation functions and are also analyzed. Different effects of the positive Q_{xn} -value neutron transfer in the fusion enhancement are revealed in the relatively close reactions $^{32}\text{S}+^{94,96}\text{Zr}$ and $^{40}\text{Ca}+^{94,96}\text{Zr}$.

PACS numbers: 25.70.Jj, 24.10.-i, 24.60.-k

Key words: sub-barrier capture (fusion), nucleon transfer, quantum diffusion approach

I. INTRODUCTION

The nuclear deformation effects are identified as playing a major role in the magnitude of the sub-barrier fusion (capture) cross sections [1, 2]. There are several experimental evidences which confirm the straightforward influence of nuclear deformation on the fusion. If the target nucleus is prolate in the ground state, the Coulomb field on its tips is lower than on its sides. Thus, the capture or fusion probability increases at energies below the barrier corresponding to the spherical nuclei.

The dynamics of neutron transfer-mediated sub-barrier capture and fusion is not yet revealed [2]. The cross section enhancement in the sub-barrier fusion of $^{58}\text{Ni}+^{64}\text{Ni}$, with respect to $^{58}\text{Ni}+^{58}\text{Ni}$, [3] is interpreted in Ref. [4] as a kinematic effect due to the positive Q_{2n} -value of the ground-state-to-ground-state two-neutron transfer ($2n$ -transfer) channel. A correlation is observed between considerable sub-barrier fusion enhancement and positive Q_{xn} -values for neutron transfer in the reactions $^{40}\text{Ca}+^{94,96}\text{Zr}$ [5–7], and $^{40}\text{Ca}+^{116,124,132}\text{Sn}$ [8, 9].

The importance of neutron transfer with positive Q_{xn} -values in nuclear fusion (capture) originates from the fact that neutrons are insensitive to the Coulomb barrier and their transfer starts at quite larger separations, before the projectile is captured by target-nucleus. It is generally thought that the sub-barrier capture (fusion) cross section increases because of the neutron transfer [5–20]. However, the reduced excitation functions for the reactions $^{16,17,18}\text{O}+^A\text{Sn}$ ($A=112,116-120,122,124$) [21], scaled to remove the effects of smoothly varying barrier parameters, do not show any strong dependence on the mass number of target or projectile. The relative changes are within a factor two and are not correlated with the positive Q_{xn} -values of neutron-transfer channels in these reactions. As shown in Ref. [22], the neutron transfer channels with positive Q_{xn} -value weakly influence the capture (fusion) cross section in the $^{60}\text{Ni}+^{100}\text{Mo}$ reaction at sub-barrier energies. In the reactions $^{40}\text{Ca}+^{116,124}\text{Sn}$ ($Q_{2n} > 0$) and $^{132}\text{Sn},^{130}\text{Te}+^{58,64}\text{Ni}$ ($Q_{2n} > 0$) at energies above and a few MeV below the Coulomb barrier, the effect of transfer channels on the capture (fusion) is demonstrated to be very weak with no significant differences observed in the reduced excitation functions [8, 23]. In comparison with the $^{16}\text{O}+^{76}\text{Ge}$ reaction [24], the fusion enhancement due to the positive Q_{2n} -value is not revealed in the $^{18}\text{O}+^{74}\text{Ge}$ reaction.

It is presently not clear why the neutron transfers with positive Q_{xn} -values play a deci-

sive role in the fusion reactions $^{40}\text{Ca}+^{48}\text{Ca}$, $^{58}\text{Ni}+^{64}\text{Ni}$, $^{40}\text{Ca}+^{94,96}\text{Zr}$, $^{40}\text{Ca}+^{116,124,132}\text{Sn}$ and weakly influence the fusion reactions $^{58,64}\text{Ni}+^{132}\text{Sn}$, $^{58,64}\text{Ni}+^{130}\text{Te}$, $^{60}\text{Ni}+^{100}\text{Mo}$, $^{18}\text{O}+^{74}\text{Ge}$, $^{18}\text{O}+^A\text{Sn}$ [2, 25]. Although the enhancement appears to be related to the existence of large positive Q_{xn} -values for neutron transfer, it is not proportional to the magnitudes of those Q_{xn} -values, which are larger for $^{40}\text{Ca}+^{96}\text{Zr}$ [$^{40}\text{Ca}+^{132}\text{Sn}$ or $^{40}\text{Ca}+^{124}\text{Sn}$] than for $^{40}\text{Ca}+^{94}\text{Zr}$ [$^{40}\text{Ca}+^{124}\text{Sn}$ or $^{40}\text{Ca}+^{116}\text{Sn}$]. The sub-barrier enhancements are similar in these reactions. So, the influence of neutron transfer on the capture process is not trivial to be easily explained.

The quantum diffusion approach [26–30] was applied to study the role of the neutron transfer with positive Q_{xn} -value in the capture (fusion) reactions at sub-, near- and above-barrier energies. A good agreement of the theoretical calculations with the experimental data was demonstrated. As found, the change of the capture cross section after the neutron transfer occurs due to the change of the deformations of nuclei [26–30]. Thus, the effect of the neutron transfer is an indirect influence of the quadrupole deformation. As demonstrated in Ref. [27], the neutron transfer can weakly influence or even suppress the capture (fusion) cross section in some reactions.

Applying the quantum diffusion approach [26–30] (Sect. IV), the universal fusion function representation [31, 32] (Sect. II), and capture probabilities extracted from the experimental excitation functions (Sect. III), we try to answer the question how the neutron transfer influence the sub-barrier capture cross section in the reactions $^{32}\text{S}+^{90,94,96}\text{Zr}$, $^{36}\text{S}+^{90,96}\text{Zr}$, $^{40}\text{Ca}+^{90,94,96}\text{Zr}$, and $^{48}\text{Ca}+^{90,96}\text{Zr}$ at near and sub-barrier energies. We will show why the influence of positive Q_{xn} -value neutron transfer is completely different in the relatively close reactions $^{32}\text{S}+^{94,96}\text{Zr}$ and $^{40}\text{Ca}+^{94,96}\text{Zr}$.

II. EXPERIMENTAL REDUCED CAPTURE CROSS SECTIONS

To analyze the capture cross sections in the reactions with different Coulomb barrier heights V_b and radius R_b calculated in the case of spherical nuclei, it is useful to compare not the excitation functions, but the dependence of the dimensionless quantities $2E_{c.m.}\sigma_{cap}(E_{c.m.})/(\hbar\omega_b R_b^2)$ versus $(E_{c.m.} - V_b)/(\hbar\omega_b)$ or $(E_{c.m.} - V_b)$ [31, 32]. Here, ω_b and μ are the frequency of an inverted oscillator approximated the barrier and the reduced mass of the system, respectively. In the reactions, where the capture and fusion cross sections

coincide, the comparison of experimental data with the universal fusion function [31, 32] allows us to conclude about the role of static deformations of the colliding nuclei and the nucleon transfer between them in the capture cross section. Indeed, the universal function disregards these effects.

For the reactions $^{40}\text{Ca}+^{90}\text{Zr}$, $^{48}\text{Ca}+^{90,96}\text{Zr}$, and $^{36}\text{S}+^{90,96}\text{Zr}$, with almost spherical nuclei and without neutron transfer [the negative Q_{xn} -values], the experimental cross sections are rather close and fall with the same rate like the universal fusion function (Fig. 1). For the reactions $^{40}\text{Ca}+^{94,96}\text{Zr}$ with the neutron transfer [the positive Q_{xn} -values], one can see that the reduced cross sections strongly deviate from the universal function in contrast to the reactions $^{40}\text{Ca}+^{90}\text{Zr}$, $^{36}\text{S}+^{90,96}\text{Zr}$, $^{48}\text{Ca}+^{90,96}\text{Zr}$, where the neutron transfer is suppressed.

In the reactions $^{32}\text{S}+^{90,94,96}\text{Zr}$ with strongly deformed projectile ^{32}S (Fig.1), the deviations from the universal function are mainly caused by the static deformation effects. In spite of the Q_{xn} -values for the neutron transfer range from the negative [$^{32}\text{S}+^{90}\text{Zr}$] to large and positive values [$^{32}\text{S}+^{94,96}\text{Zr}$], the reduced capture (fusion) cross sections appear to be almost the same. So, we observe the strong and weak influence of neutron transfer on the capture cross sections in the reactions $^{40}\text{Ca}+^{94,96}\text{Zr}$ and $^{32}\text{S}+^{94,96}\text{Zr}$, respectively.

III. CAPTURE PROBABILITIES EXTRACTED FROM EXPERIMENTAL CAPTURE EXCITATION FUNCTIONS

Shifting the energy by the rotational energy $E_R(J) = \frac{\hbar^2 J(J+1)}{2\mu R_b^2}$ [36], one can approximate the angular momentum J dependence of the transmission (capture) probability $P_{cap}(E_{c.m.}, J)$, at a given $E_{c.m.}$:

$$P_{cap}(E_{c.m.}, J) \approx P_{cap}(E_{c.m.} - E_R(J), J = 0). \quad (1)$$

If we use the formula for the capture cross section, convert the sum over the partial waves J into an integral, and express J by the variable $E = E_{c.m.} - E_R(J)$, we obtain the following simple expression:

$$\sigma_{cap}(E_{c.m.}) = \frac{\pi R_b^2}{E_{c.m.}} \int_0^{E_{c.m.}} dE P_{cap}(E, J = 0). \quad (2)$$

Multiplying this equation by $E_{c.m.}/(\pi R_b^2)$ and differentiating over $E_{c.m.}$, one obtains [36]:

$$P_{cap}(E_{c.m.}, J = 0) = \frac{1}{\pi R_b^2} \frac{d[E_{c.m.}\sigma_{cap}(E_{c.m.})]}{dE_{c.m.}}. \quad (3)$$

One can see that $\frac{d[E_{c.m.}\sigma_{cap}(E_{c.m.})]}{dE_{c.m.}}$ has a meaning of the s -wave transmission in the entrance channel. Therefore, the s -wave capture probability can be extracted with a satisfactory accuracy from the experimental capture cross sections $\sigma_{cap}(E_{c.m.})$ at energies near and below the Coulomb barrier. Note that at energies considered the dependence of the Coulomb barrier radius on the angular momentum is very weak.

The extraction method just described requires some procedure to smooth the experimental data since the values of $E_{c.m.}\sigma_{cap}(E_{c.m.})$ have error bars. We spline the experimental points of $E_{c.m.}\sigma_{cap}(E_{c.m.})$ by the Bézier parametric curve [37].

In Figs. 2 and 3, the extracted capture probabilities $P_{cap}(E, J = 0)$ demonstrate the influence of nucleon transfer on the capture (fusion) excitation function. In the reactions $^{40}\text{Ca}+^{90}\text{Zr}$ and $^{48}\text{Ca}+^{90,96}\text{Zr}$ with the negative Q_{xn} -values for nucleon transfer, the capture probability exhibits a steep falloff of the probability at low energies. However, the first derivatives of $P_{cap}(E, J = 0)$ are almost the same. Conversely, the reactions $^{40}\text{Ca} + ^{94,96}\text{Zr}$ have positive Q_{xn} -values for neutron transfer. This leads to the smaller slope of probability functions at sub-barrier energies. The capture probabilities in the reactions $^{40}\text{Ca}+^{94,96}\text{Zr}$ are close to each other.

Since the nucleus ^{36}S is spherical, the slopes of functions $P_{cap}(E, J = 0)$ for the reactions $^{36}\text{S}+^{90,96}\text{Zr}$ are larger than those for the reactions $^{32}\text{S}+^{94,96}\text{Zr}$ and $^{32}\text{S}+^{90}\text{Zr}$ with the strongly deformed ^{32}S . The slopes of functions $P_{cap}(E, J = 0)$ are rather similar (Fig. 3) in the $^{32}\text{S}+^{90}\text{Zr}$ reaction with the negative Q_{xn} -values for neutron transfer and in the reactions $^{32}\text{S}+^{94,96}\text{Zr}$ with the positive Q_{xn} -values for neutron transfer. Thus, the enhancement of capture probability in these reactions has the same origin. It arises due to the large static deformations of nuclei $^{32,34}\text{S}$ and the neutron transfer is not responsible for the capture (fusion) enhancement.

As follows from the extracted capture probabilities, the experimental normalizations of the cross sections are different in the reactions $^{32}\text{S}+^{90,94,96}\text{Zr}$ and $^{36}\text{S}+^{90,96}\text{Zr}$. One should think about the experimental reasons for such deviations.

IV. CALCULATIONS WITHIN THE QUANTUM DIFFUSION APPROACH

In the quantum diffusion approach [26–30, 38] the collisions of nuclei are described with a single relevant collective variable: the relative distance between the colliding nuclei. This

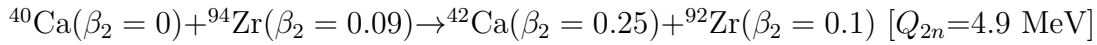
approach takes into consideration the fluctuation and dissipation effects in collisions of heavy ions which model the coupling with various channels (for example, the non-collective single-particle excitations, low-lying collective dynamical modes of the target and projectile). We have to mention that many quantum-mechanical and non-Markovian effects accompanying the passage through the potential barrier are taken into consideration in our formalism [26–30, 38]. The nuclear deformation effects are taken into account through the dependence of the nucleus-nucleus potential on the deformations and mutual orientations of the colliding nuclei. To calculate the nucleus-nucleus interaction potential $V(R)$, we use the procedure presented in Refs. [26–30, 38]. For the nuclear part of the nucleus-nucleus potential, the double-folding formalism with the Skyrme-type density-dependent effective nucleon-nucleon interaction is used. With this approach many heavy-ion capture reactions at energies above and well below the Coulomb barrier have been successfully described [26–30, 38].

Following the hypothesis of Ref. [4], we assume that the sub-barrier capture in the reactions under consideration mainly depends on the two-neutron transfer with the positive Q_{2n} -value. Our assumption is that, just before the projectile is captured by the target-nucleus (just before the crossing of the Coulomb barrier) which is a slow process, the $2n$ -transfer ($Q_{2n} > 0$) transfer occurs and leads to the population of the first excited collective state in the recipient nucleus [39] (the donor nucleus remains in the ground state). The absolute values of the quadrupole deformation parameters β_2 in 2^+ state of even-even deformed nuclei are taken from Ref. [40]. For the nuclei deformed in the ground state, the β_2 in the first excited collective state is similar to that in the ground state. For the double magic and semi-magic nuclei, we take $\beta_2 = 0$ in the ground state.

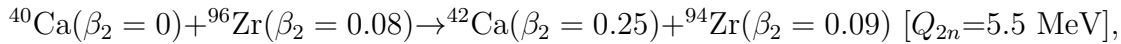
The motion to N/Z equilibrium starts in the system before the capture occurs because it is energetically favorable in the dinuclear system in the vicinity of the Coulomb barrier. For the reactions under consideration, the average change of mass asymmetry is related to the two-neutron transfer. In these reactions, $Q_{2n} > Q_{1n}$ and during the capture the $2n$ -transfer is more probable than $1n$ -transfer. After the $2n$ -transfer the mass numbers, the deformation parameters of the interacting nuclei, and, correspondingly, the height V_b and shape of the Coulomb barrier change. Then one can expect an enhancement or suppression of the capture. If after the neutron transfer the deformations of interacting nuclei increase (decrease), the capture probability increases (decreases). If after the transfer the deformations of interacting nuclei do not change, there is no effect of the neutron transfer on the capture. This scenario

was verified in the description of many reactions [26–30, 38].

In Fig. 4 one can see a good agreement between the calculated and the experimental capture cross sections in the reactions $^{40}\text{Ca}+^{94,96}\text{Zr}$ with the positive Q values for neutron transfer and in the reactions $^{40}\text{Ca}+^{90}\text{Zr}$, $^{48}\text{Ca}+^{90,96}\text{Zr}$ with negative Q -values for neutron transfer. The theoretical calculations describe the strong deviation of the slopes of excitation functions in the reactions $^{40}\text{Ca}+^{94,96}\text{Zr}$ with positive Q -values for neutron transfer from those in the reactions $^{40}\text{Ca}+^{90}\text{Zr}$, $^{48}\text{Ca}+^{90,96}\text{Zr}$, where the neutron transfers are suppressed because of negative Q -values. This means that the observed capture enhancements in the reactions $^{40}\text{Ca}+^{94,96}\text{Zr}$ at sub-barrier energies are related to the two-neutron transfer effect. After $2n$ -transfer in the reactions



and



the deformation of the light nucleus strongly increases and, thus, the height of the Coulomb barrier decreases and the capture cross section becomes larger (Fig. 4). So, because of the neutron-transfer effect the reactions $^{40}\text{Ca}+^{94,96}\text{Zr}$ show large sub-barrier enhancements with respect to the reactions $^{48}\text{Ca}+^{90,96}\text{Zr}$ and $^{40}\text{Ca}+^{90}\text{Zr}$. One can see in Fig.5 that with decreasing the sub-barrier energy the cross sections with and without two-neutron transfer strongly deviate. The slopes of the excitation functions in the reactions $^{40}\text{Ca}+^{94,96}\text{Zr}$ are almost the same because in both cases after the neutron transfer the nuclei have similar deformations. The relative enhancement of the sub-barrier fusion cross sections in the reactions $^{40}\text{Ca}+^{94,96}\text{Zr}$ with respect to those in the reactions $^{48}\text{Ca}+^{90,96}\text{Zr}$ and $^{40}\text{Ca}+^{90}\text{Zr}$ is mainly related to the deformation of ^{42}Ca in the 2^+ state. Thus, the observed capture enhancement at sub-barrier energies in the reactions $^{40}\text{Ca}+^{94,96}\text{Zr}$ is purely related to the transfer effects.

Since the sub-barrier enhancements are surprisingly similar for the two reactions $^{40}\text{Ca}+^{94,96}\text{Zr}$ with different positive Q -values for neutron transfer, one can assume that the absolute value of the positive Q -value is rather unimportant for the capture following transfer. If the transfer is energetically favorable it occurs during the capture process. In this case the transfer influences the capture (fusion) [or the height and width of the Coulomb barrier] through the change of the isotopic composition of interacting nuclei and, correspondingly, through the change of their deformations.

Figure 6 shows the capture (fusion) excitation functions for the reactions $^{32}\text{S}+^{90,94,96}\text{Zr}$

and $^{36}\text{S}+^{90,96}\text{Zr}$. The Q_{2n} -values for the $2n$ -transfer processes are positive (negative) for the reactions $^{32}\text{S}+^{94,96}\text{Zr}$ ($^{32}\text{S}+^{90}\text{Zr}$, $^{36}\text{S}+^{90,96}\text{Zr}$). After the $2n$ -transfer (before the capture) in the reactions (Figs. 4 and 6)

$$^{32}\text{S}(\beta_2 = 0.31)+^{94}\text{Zr}(\beta_2 = 0.09)\rightarrow^{34}\text{S}(\beta_2 = 0.25)+^{92}\text{Zr}(\beta_2 = 0.1) [Q_{2n}=5.1 \text{ MeV}]$$

and

$$^{32}\text{S}(\beta_2 = 0.31)+^{96}\text{Zr}(\beta_2 = 0.08)\rightarrow^{34}\text{S}(\beta_2 = 0.25)+^{94}\text{Zr}(\beta_2 = 0.09) [Q_{2n}=5.7 \text{ MeV}],$$

the deformation of S slightly decreases and the values of the corresponding Coulomb barriers slightly increase. As a result, the transfer weakly suppresses the capture process at the sub-barrier energies. This suppression becomes stronger with decreasing energy. One can see in Fig. 5 that at energies above, near, and below the Coulomb barrier the cross sections with and without two-neutron transfer are almost similar in the reactions $^{32}\text{S}+^{94,96}\text{Zr}$. The relative enhancement of the sub-barrier fusion cross sections in the reactions $^{32}\text{S}+^{94,96}\text{Zr}$ with respect to that in the reactions $^{36}\text{S}+^{90,96}\text{Zr}$ is mainly related to the deformation of ^{34}S in the 2^+ state. With respect to the reactions $^{36}\text{S}+^{94,96}\text{Zr}$ the enhancements of cross sections in the reactions $^{32}\text{S}+^{94,96}\text{Zr}$ and $^{32}\text{S}+^{90}\text{Zr}$ are similar because of the close deformations of interacting nuclei after neutron transfer. So, the observed capture enhancement at sub-barrier energies in the reactions $^{32}\text{S}+^{94,96}\text{Zr}$ and $^{32}\text{S}+^{90}\text{Zr}$ is not related to the transfer effects but to the direct static deformation effects.

V. SUMMARY

The quantum diffusion approach, the universal fusion function representation, the extracted capture probabilities from the experimental excitation functions are applied to study the role of the neutron transfer with positive Q_{xn} -values in the capture (fusion) reactions $^{40}\text{Ca}+^{94,96}\text{Zr}$ and $^{32}\text{S}+^{94,96}\text{Zr}$. We found that the change of the capture (fusion) cross section after the two-neutron transfer occurs due to the change of the deformations of nuclei. When after the neutron transfer the deformations of nuclei strongly (weakly) change, the neutron transfer strongly (weakly) influences the fusion cross section. We clearly showed that the neutron transfer effects on the excitation functions in the reactions $^{40}\text{Ca}+^{94,96}\text{Zr}$ and $^{32}\text{S}+^{94,96}\text{Zr}$ are completely different. The calculations pointed a strong increase of the fusion enhancement due to the neutron transfer for the systems with the spherical acceptor-nuclei as in the case of the reactions $^{40}\text{Ca}+^{94,96}\text{Zr}$. In the reactions $^{32}\text{S}+^{94,96}\text{Zr}$ with the

well deformed acceptor-nucleus ^{32}S , the strong fusion enhancement arises due to the static deformation effects.

Combining all our calculations within the quantum diffusion approach, one can come to the following conclusions about the role of neutron transfer in the capture (fusion) reactions with positive Q_{xn} -values for the neutron transfer.

(a) If the acceptor-nucleus is spherical or slightly deformed (relatively strongly bound) nucleus and the donor-nucleus is the spherical or deformed nucleus, the neutron transfer may lead to the strong capture (fusion) enhancement [for example, $^{40}\text{Ca}+^{94,96}\text{Zr}$, $^{116,124,132}\text{Sn}$, ^{154}Sm , $^{58}\text{Ni}+^{64}\text{Ni}$, and $^{40}\text{Ca}+^{48}\text{Ca}$] or to the weak influence or even to the weak suppression [for example, $^{18}\text{O}+^{92}\text{Mo}$, $^{112,118,124}\text{Sn}$].

(b) If the acceptor-nucleus is strongly deformed (relatively weakly bound) nucleus and the donor-nucleus is the spherical or deformed nucleus, the neutron transfer may lead to the weak influence or even to the weak suppression [for example, $^{18}\text{O}+^{74}\text{Ge}$, $^{60}\text{Ni}+^{100}\text{Mo}$, $^{28}\text{Si}+^{142}\text{Ce}$, ^{154}Sm , and $^{32}\text{S}+^{94,96}\text{Zr}$, $^{96-100}\text{Mo}$, $^{100-104}\text{Ru}$, ^{110}Pd , ^{154}Sm , ^{208}Pb]. In these reactions with strongly deformed nuclei ^{28}Si , ^{32}S , and ^{74}Ge the fusion enhancement is caused by the static deformation effects.

Thus, the point of view that the sub-barrier capture (fusion) cross section can be weakly influenced or even suppressed because of the neutron transfer with positive Q_{xn} -values has to be carefully studied. We predict the weak neutron transfer effects in the fusion reactions $^{60,62}\text{Ni}+^{150}\text{Nd}$, $^{18}\text{O}+^{64}\text{Ni}$, $^{114,116,120,122,126}\text{Sn}$, $^{204,206}\text{Pb}$, and ^{28}Si , $^{32}\text{S}+^{116-134}\text{Sn}$, $^{148-152}\text{Sm}$. As shown with the quantum diffusion approach, the capture cross sections almost match in the reactions $^{16}\text{O}+^{52}\text{Cr}$ and $^{18}\text{O}+^{50}\text{Cr}$, $^{16}\text{O}+^{94}\text{Mo}$ and $^{18}\text{O}+^{92}\text{Mo}$, $^{16}\text{O}+^{114,120,124,126}\text{Sn}$ and $^{18}\text{O}+^{112,118,122,124}\text{Sn}$, respectively. The same reduced fusion cross sections for the reactions $^{58,60,62}\text{Ni}+^{150}\text{Nd}$ with positive Q_{2n} -values [$Q_{2n}=8.2, 6.0, 4.1$ MeV, respectively] are predicted.

G.G.A. and N.V.A. acknowledge the partial support from the Alexander von Humboldt-Stiftung (Bonn). This work was supported by RFBR and NSFC. The IN2P3(France)-JINR(Dubna) Cooperation Programme is gratefully acknowledged.

[1] L.F. Canto, P.R.S. Gomes, R. Donangelo, and M.S. Hussein, Phys. Rep. **424**, (2006) 1 and references therein.

- [2] B.B. Back, H. Esbensen, C.L. Jiang and K.E. Rehm, *Rev. Mod. Phys.* **86**, 317(2014) and references therein.
- [3] M. Beckerman *et al.*, *Phys. Rev. Lett.* **45** (1980) 1472; M. Beckerman, J. Ball, H. Enge, M. Salomaa, A. Sperduto, S. Gazes, A. DiRienzo, and J.D. Molitoris, *Phys. Rev. C* **23** (1981) 1581; M. Beckerman, M. Salomaa, A. Sperduto, J.D. Molitoris, and A. DiRienzo, *Phys. Rev. C* **25** (1982) 837.
- [4] R.A. Broglia, C.H. Dasso, S. Landowne, and A. Winther, *Phys. Rev. C* **27**, 2433 (1983); R.A. Broglia, C.H. Dasso, S. Landowne, and G. Pollarolo, *Phys. Lett. B* **133**, 34 (1983).
- [5] H. Timmers *et al.*, *Nucl. Phys.* **A633**, 421 (1998).
- [6] A.M. Stefanini *et al.*, *Phys. Rev. C* **76**, 014610 (2007).
- [7] A.M. Stefanini *et al.*, *Phys. Lett. B* **728**, 639 (2014).
- [8] F. Scarlassara *et al.*, *Nucl. Phys.* **A672**, 99 (2000).
- [9] J.J. Kolata *et al.*, *Phys. Rev. C* **85**, 054603 (2012).
- [10] R. Pengo *et al.*, *Nucl. Phys.* **A411**, 255 (1983).
- [11] W. Henning, F.L.H. Wolfs, J.P. Schiffer, and K.E. Rehm, *Phys. Rev. Lett.* **58**, 318 (1987).
- [12] P.H. Stelson, H.J. Kim, M. Beckerman, D. Shapira, and R.L. Robinson, *Phys. Rev. C* **41**, 1584 (1990).
- [13] R.B. Roberts *et al.*, *Phys. Rev. C* **47**, R1831 (1993).
- [14] A.M. Stefanini *et al.*, *Phys. Rev. C* **52**, R1727 (1995).
- [15] A.A. Sonzogni, J.D. Bierman, M.P. Kelly, J.P. Lestone, J.F. Liang, and R. Vandenbosch, *Phys. Rev. C* **57**, 722 (1998).
- [16] V. Tripathi *et al.*, *Phys. Rev. C* **65**, 014614 (2001).
- [17] C.L. Jiang *et al.*, *Phys. Rev. C* **82**, 041601(R) (2010).
- [18] H.Q. Zhang *et al.*, *Phys. Rev. C* **82**, 054609 (2010).
- [19] Z. Kohley *et al.*, *Phys. Rev. C* **87**, 064612 (2013).
- [20] H. M. Jia *et al.*, *Phys. Rev. C* **89**, 064605 (2014).
- [21] P. Jacobs, Z. Fraenkel, G. Mamane, and L. Tserruya, *Phys. Lett. B* **175**, 271 (1986).
- [22] F. Scarlassara *et al.*, *EPJ Web Conf.* **17**, 05002 (2011).
- [23] Z. Kohley *et al.*, *Phys. Rev. Lett.* **107**, 202701 (2011); J.F. Liang, *EPJ Web Conf.* **17**, 02002 (2011); J.F. Liang *et al.*, *Phys. Rev. C* **78**, 047601 (2008).
- [24] H.M. Jia *et al.*, *Phys. Rev. C* **86**, 044621 (2012).

- [25] C.L. Jiang *et al.*, Phys. Rev. C **89**, 051603(R) (2014).
- [26] V.V. Sargsyan, G.G. Adamian, N.V. Antonenko, and W. Scheid, Eur. Phys. J. A **45**, 125 (2010); V.V. Sargsyan, G.G. Adamian, N.V. Antonenko, W. Scheid, and H.Q. Zhang, Eur. Phys. J. A **47**, 38 (2011); J. of Phys.: Conf. Ser. **282**, 012001 (2011); EPJ Web Conf. **17**, 04003 (2011); V.V. Sargsyan, G.G. Adamian, N.V. Antonenko, W. Scheid, C.J. Lin, and H.Q. Zhang, Phys. Rev. C **85**, 017603 (2012); Phys. Rev. C **85**, 037602 (2012).
- [27] V.V. Sargsyan, G.G. Adamian, N.V. Antonenko, W. Scheid, and H.Q. Zhang, Phys. Rev. C **84**, 064614 (2011); Phys. Rev. C **85**, 024616 (2012).
- [28] V.V. Sargsyan, G.G. Adamian, N.V. Antonenko, W. Scheid, and H.Q. Zhang, *Phys. Rev. C* **86**, 014602 (2012).
- [29] V.V. Sargsyan, G.G. Adamian, N.V. Antonenko, W. Scheid, and H.Q. Zhang, *Eur. Phys. J. A* **49**, 54 (2013).
- [30] V.V. Sargsyan, G. Scamps, G.G. Adamian, N.V. Antonenko, and D. Lacroix, Phys. Rev. C **88**, 064601 (2013).
- [31] L.F. Canto, P.R.S. Gomes, J. Lubian, L.C. Chamon, and E. Crema, J. Phys. G **36**, 015109 (2009).
- [32] L.F. Canto, P.R.S. Gomes, J. Lubian, L.C. Chamon, and E. Crema, Nucl. Phys. **A821**, 51 (2009).
- [33] A.M. Stefanini *et al.*, Phys. Rev. C **73**, 034606 (2006).
- [34] A.M. Stefanini *et al.*, Phys. Rev. C **62**, 014601 (2000).
- [35] G. Montagnoli, *et al.*, Phys. Rev. C **85**, 024607 (2012).
- [36] A.B. Balantekin, S.E. Koonin, and J.W. Negele, Phys. Rev. C **28**, 1565 (1983); A.B. Balantekin and P.E. Reimer, Phys. Rev. C **33**, 379 (1986); A.B. Balantekin, A.J. DeWeerd, and S. Kuyucak, Phys. Rev. C **54**, 1853 (1996).
- [37] P. Henrici, *Essentials of numerical analysis*, (John Wiley & Sons, Inc. New York, NY, USA, 1982).
- [38] R.A. Kuzyakin, V.V. Sargsyan, G.G. Adamian, N.V. Antonenko, E.E. Saperstein, and S.V. Tolokonnikov, Phys. Rev. C **85**, 034612 (2012).
- [39] S. Szilner *et al.*, Phys. Rev. C **76**, 024604 (2007); S. Szilner *et al.*, Phys. Rev. C **84**, 014325 (2011).
- [40] S. Raman, C.W. Nestor, Jr, and P. Tikkanen, At. Data Nucl. Data Tables **78**, 1 (2001).

Figures

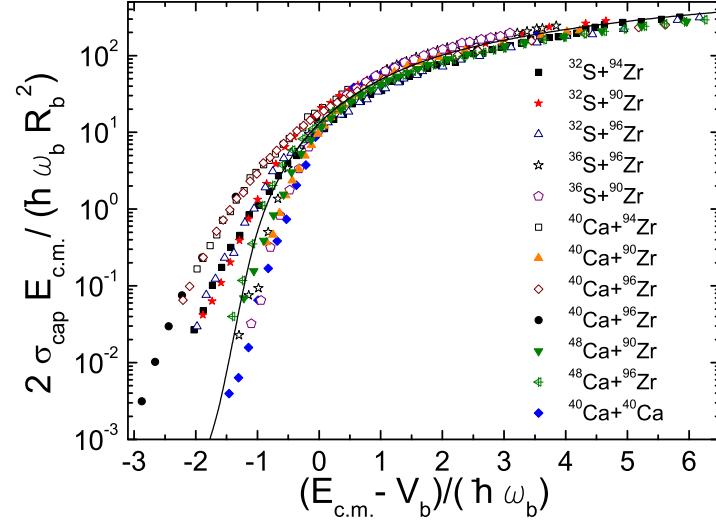


FIG. 1: (Color online) Comparison of the universal fusion function (solid line) with the experimental values [5–7, 18, 20, 33–35] (symbols) of $\frac{2E_{c.m.}}{\hbar\omega_b R_b^2} \sigma_{cap}(E_{c.m.})$ vs $\frac{E_{c.m.} - V_b}{\hbar\omega_b}$ for the reactions indicated.

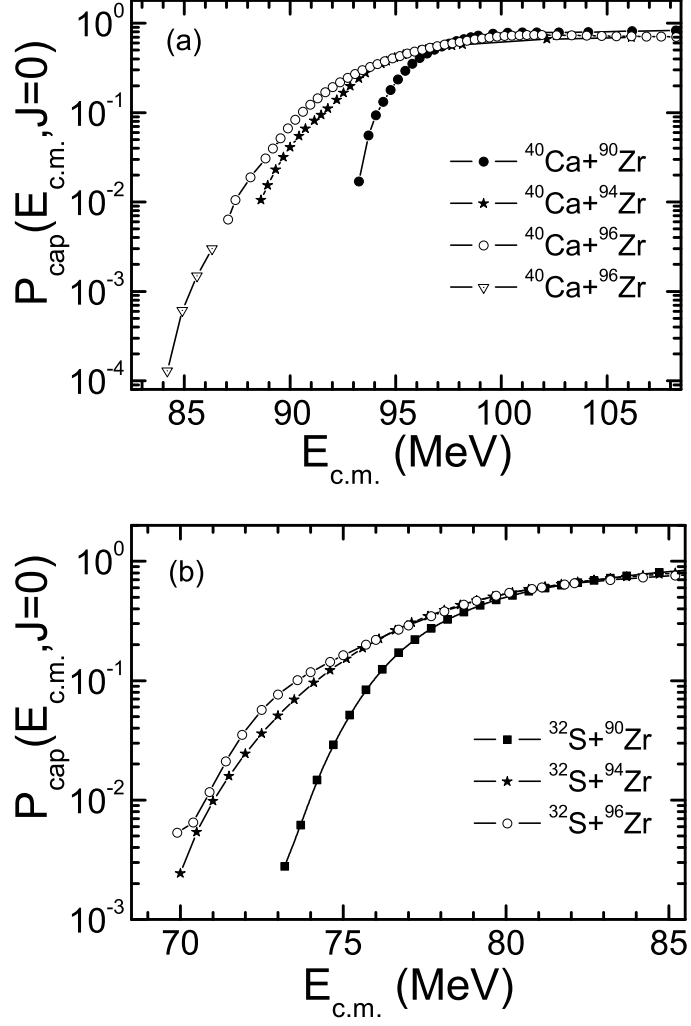


FIG. 2: The extracted s -wave capture probabilities for the reactions indicated by employing Eq. (3) [symbols connected by lines]. The used experimental capture (fusion) excitation functions are from Refs. [5–7, 18, 20].

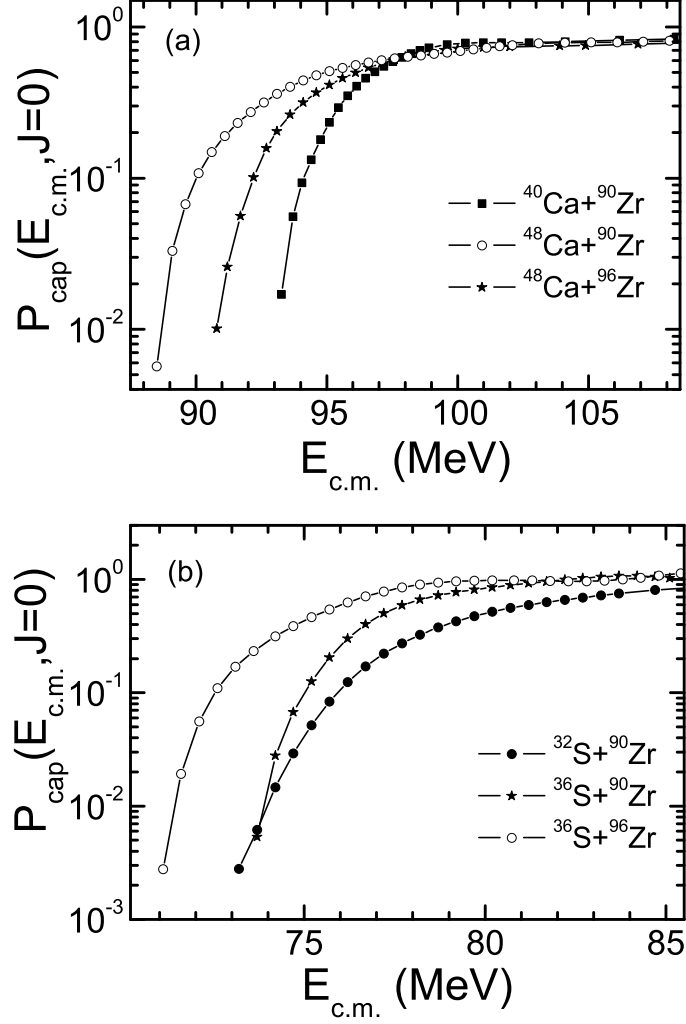


FIG. 3: The extracted s -wave capture probabilities for the reactions indicated by employing Eq. (3) [symbols connected by lines]. The used experimental capture (fusion) excitation functions are from Refs. [5, 18, 33, 34].

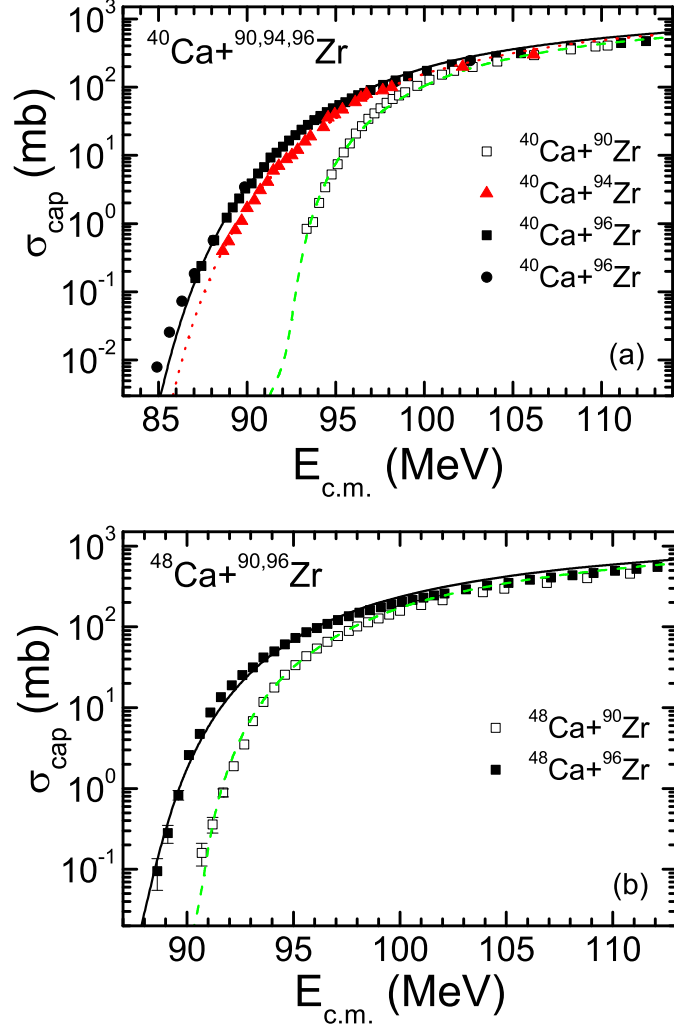


FIG. 4: (Color online) The calculated capture cross sections vs $E_{\text{c.m.}}$ for the reactions (a) $^{40}\text{Ca} + ^{96}\text{Zr}$ (solid line), $^{40}\text{Ca} + ^{94}\text{Zr}$ (dotted line), $^{40}\text{Ca} + ^{90}\text{Zr}$ (dashed line) and (b) $^{48}\text{Ca} + ^{96}\text{Zr}$ (solid line), $^{48}\text{Ca} + ^{90}\text{Zr}$ (dashed line). The experimental data (symbols) are from Refs. [5–7, 33].

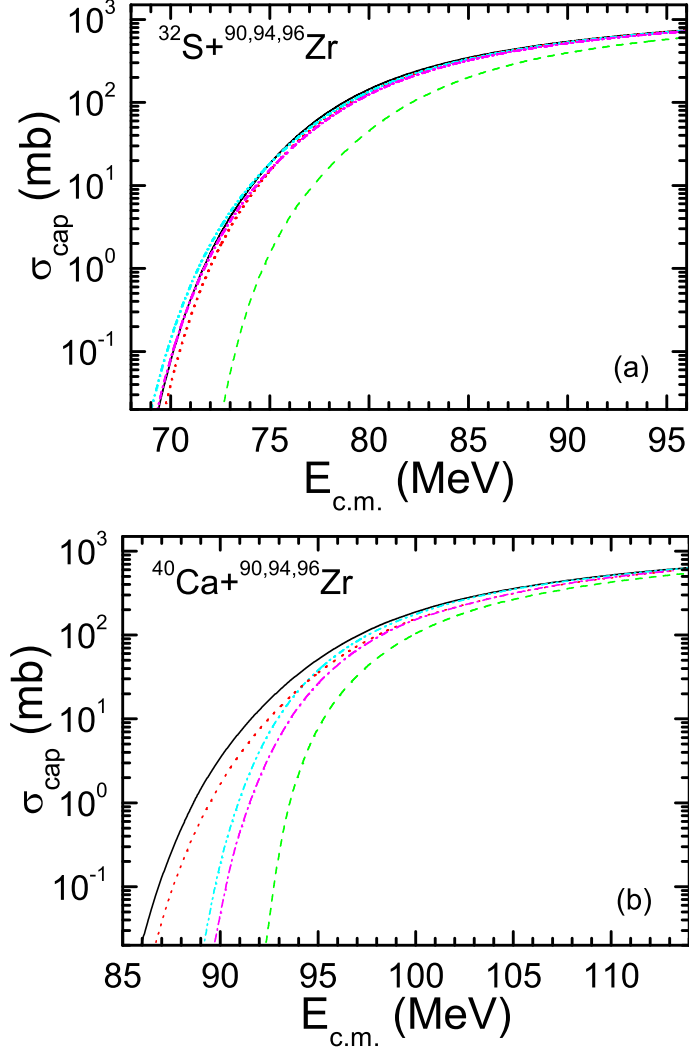


FIG. 5: (Color online) The calculated capture cross sections vs $E_{c.m.}$ for the reactions (b) $^{40}\text{Ca}+^{96}\text{Zr}$ (solid line), $^{40}\text{Ca}+^{94}\text{Zr}$ (dotted line), $^{40}\text{Ca}+^{90}\text{Zr}$ (dashed line) and (a) $^{32}\text{S}+^{96}\text{Zr}$ (solid line), $^{32}\text{S}+^{94}\text{Zr}$ (dotted line), $^{32}\text{S}+^{90}\text{Zr}$ (dashed line). For the reactions $^{32}\text{S},^{40}\text{Ca}+^{96}\text{Zr}$ and $^{32}\text{S},^{40}\text{Ca}+^{94}\text{Zr}$, the capture cross sections calculated without taking into consideration the neutron transfer are shown by dash-dot-dotted and dash-dotted [it is matched with solid line in the part (a)] lines, respectively.

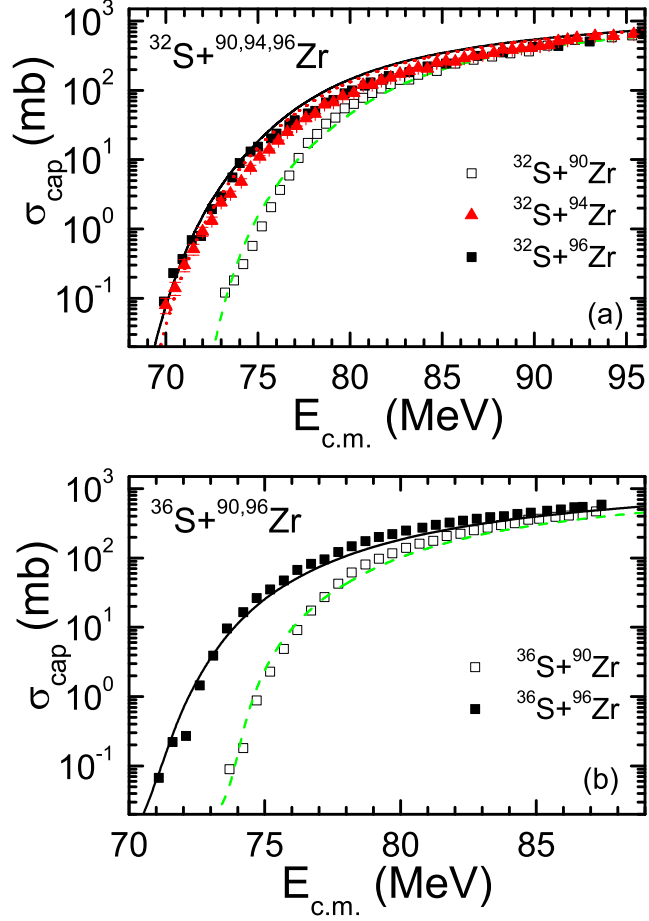


FIG. 6: (Color online) The calculated capture cross sections vs $E_{c.m.}$ for the reactions (a) $^{32}\text{S}+^{96}\text{Zr}$ (solid line), $^{32}\text{S}+^{94}\text{Zr}$ (dotted line), $^{32}\text{S}+^{90}\text{Zr}$ (dashed line) and (b) $^{36}\text{S}+^{96}\text{Zr}$ (solid line), $^{36}\text{S}+^{90}\text{Zr}$ (dashed line). The experimental data (symbols) are from Refs. [18, 20, 34].